

Deformation mechanisms in the core of a fold:
Implications for fold-tightening mechanisms - Canyon
Range Syncline in the Sevier Fold-Thrust Belt, Utah

By: Bryn Benford

Advisor: Dr. Zeshan Ismat

15 April 2005

顶级地质论坛: <http://bbs.3s01.com/>

Bryn Ashley Benford
Dept. of Earth & Environmental Sci.
Structural Geology
Graduation Date: 5/15/05
Project Submitted: 4/15/05

Abstract

Cores of folds often hold critical clues to an entire fold's evolutionary history. Fold shape adjustments often begin in the fold core and continue to take place there because this is the region where space problems predominantly arise. Retrodeforming a fold to unravel its kinematic history can often be problematic because many stages of the deformation may not be adequately recorded in the rocks. For example, in the plastic regime, evidence for early stages of deformation may be masked as a result of recrystallization. Folds that form in the elasto-frictional (EF) regime, by fracturing and cataclastic flow, may preserve a fold's history more completely; younger fractures simply cross-cut older fractures rather than erase the previous stages of deformation.

The Canyon Range (CR) syncline, part of an internal thrust sheet in the central Utah segment of the Sevier fold-thrust belt (FTB), tightened under shallow crustal conditions (at depths <5 km), so the fold evolved within the EF regime, predominantly by cataclastic flow. As the syncline tightened, synorogenic conglomerates eroding from an adjacent anticline to its west were deposited in its core. Together with the host beds, these synorogenic conglomerates were folded by cataclastic flow. The cataclasized rocks in the conglomerate and adjacent older beds interact minimally, even though both are intensely fractured. The rheology and type of cataclasis that took place in the two types of rocks are quite different; the conglomerates have a significant amount of matrix whereas the older beds essentially have none and the boundary between them is not significantly disturbed. In addition to the complex cataclasis that took place in the core, several types of macro-scale structures, such as out of the core thrusts and parasitic folds were formed. Some of these structures crosscut lithologic boundaries while others are confined to individual rock types.

The fractures (micro- and meso-scales), conglomerates, small scale folds and out-of-the-core thrusts (all within the core of the fold) were carefully analyzed in order to incrementally retrodeform the CR syncline. My analysis shows that the hinge of the CR syncline migrated and that there was a significant amount of deformation parallel to the fold hinge (i.e. non-plane strain).

Acknowledgements

I would first like to thank my advisor, Dr. Zeshan Ismat; she has been absolutely amazing in this two-year adventure. She was always available for me to bounce off my crazy ideas and to try out new ideas. I have learned so much through her and I would never have come so far with this project without her. I will truly miss having her as an advisor and as a friend.

I would also like to thank the Committee on Grants for supplying the funding for me to go to Utah to work in the field and to make all of the thin sections that I needed.

Thank you to the members of my defense committee – Dr. Roger Thomas, Dr. Rob Sternberg, and Dr. Don Fisher. Thank you for taking the time to learn about my research. It means very much to me.

Finally, I would like to thank the Earth and Environment Department. They have made my experience here at Franklin and Marshall wonderful. The professors and the alumnae together create a powerful learning environment. I am proud to be a part of it.

Table of Contents

	Page
Abstract.	ii
Acknowledgements.	iii
Table of Contents.	iv
List of Figures.	v
Introduction.	1
Geology.	6
Regional Geology.	6
Stratigraphy of Canyon Range Thrust Sheet.	7
Local Geology.	9
Canyon Range Syncline.	10
Cataclastic Flow.	11
Data Collection.	12
Macro-scale Structures.	12
Meso-scale Structures.	15
Micro-scale Structures.	19
Data Analysis.	22
Macro-scale Structures.	22
Meso-scale Structures.	24
Micro-scale Structures.	29
Interpretation.	36
Macro-scale Interpretation.	36
Meso-scale Interpretation.	37
Micro-scale Interpretation.	45
Discussion.	46
Future Work.	47
Conclusions.	47
References.	50
Appendix.	52

List of Figures

	Page
Figure 1. Mechanisms for fold-tightening.	2
Figures 2. Site location.	3
Figures 3. Kinematic history.	4
Figure 4. Stratigraphy	8
Figure 5. Fracture Criterion and Cataclasis.	13
Figure 6. Aerial photograph and topographic map of field area	14
Figure 7. Aerial photographs of CR syncline	16
Figure 8. Photograph of location of sites	17
Figure 9. Structures in the core	18
Figure 10. Fractures in CR conglomerate	18
Figure 11. S-fold in east limb	20
Figure 12. Photomicrographs in plane light and dark field	21
Figure 13. Hinge migration model.	23
Figure 14. Down-plunge projection and thickness changes.	25
Figure 15. DPP with change in area.	25
Figure 16. Reches fractures.	26
Figure 17. Stereograms of fracture sets.	27
Figure 18. Stereograms of small-scale folds.	28
Figure 19. Stereograms of motion planes.	30
Figure 20. Feldspar grains.	31
Figure 21. Grain shape/size data.	33
Figure 22. Micro-scale cataclasite zone.	34
Figure 23. Photomicrographs.	34
Figure 24. Fracturing of grains.	35
Figure 25. Model of evolution of fracture sets.	38
Figure 26. Differing styles of ductile deformation.	41
Figure 27. Model of quartzite layers' hinges.	43
Figure 28. Total grain area versus amount of grains.	44
Figure 29. SEM structures.	49

Introduction

The core of a fold holds critical clues to the kinematic history of a folded region. As a fold tightens, space problems develop within the core; a fold responds by changing its overall shape with different types of accommodating structures, so study of this area can reveal much about a fold's history. Typically, the fold changes its shape by: (1) thickening in the hinge region and thinning in the limbs, (2) hinge migration, (3) shortening in the inner arc and extension in the outer arc of the fold, and (4) temporal and spatial variations in bed-parallel flexural slip throughout the fold (Fig. 1). I have conducted detailed analyses of the core of the Canyon Range syncline as a case study in order to better understand deformation associated with fold-tightening.

The Canyon Range syncline is part of the folded Canyon Range thrust sheet, an internal thrust sheet in the central Utah segment of the Sevier FTB (Fig. 2). The Canyon Range thrust sheet was continuously reactivated by younger thrusts, below and in front of the Canyon Range thrust (Fig. 3a). The Canyon Range thrust sheet folded into a more or less north-south trending anticline-syncline pair due to this continued reactivation; the east limb of the anticline and the west limb of the syncline are a common limb. Synorogenic conglomerates, much of which were shed from the adjoining anticline, were deposited into the core of the syncline during fold-tightening. The conglomerates were also folded and reworked as the thrust sheet fold tightened (Fig. 3b). Much of the fold-tightening took place under shallow crustal conditions, i.e. within the elasto-frictional regime, so deformation progressed primarily by fracturing and cataclastic flow.

The Canyon Range syncline is an ideal place to study fold-tightening mechanisms for several reasons. First, this portion of the fold is very well exposed. Second, most of its fold-

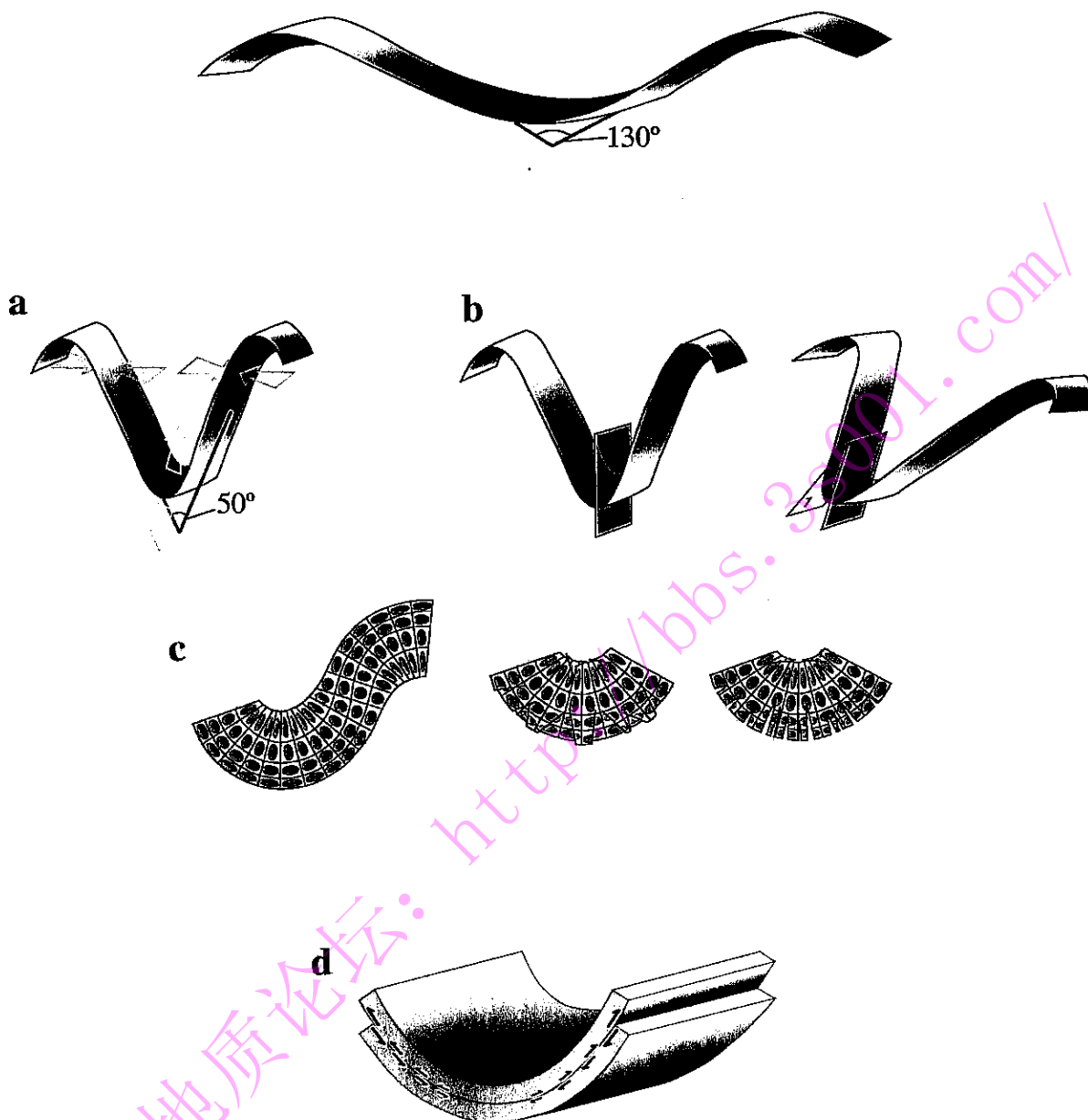
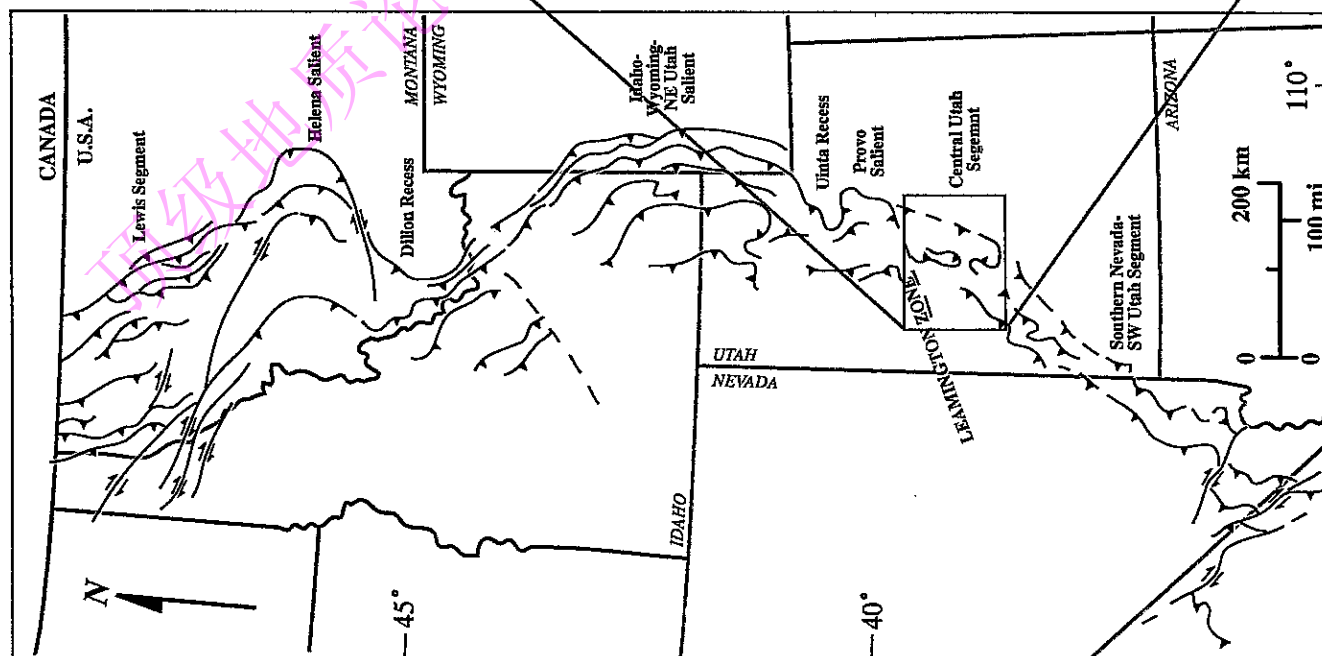


Figure 1. Once a certain interlimb angle is reached (depending on bed thickness, lithology, etc.), other mechanisms are required to continue fold tightening, mainly by adjusting the shape of the fold. The fold shape may change by: (a) thickening in the hinge region and thinning in the limbs, (b) hinge migration, (c) shortening in the inner arc and extension in the outer arc, and d) variable amounts of bed-parallel flexural slip in different parts of the fold. In part (b), the hinge surface labeled “1” shows the location of the original hinge. Note how it migrates into the left limb with continued fold-tightening. The location of the new hinge surface is labeled with a “2” (from Ismat, 1999).

a



b

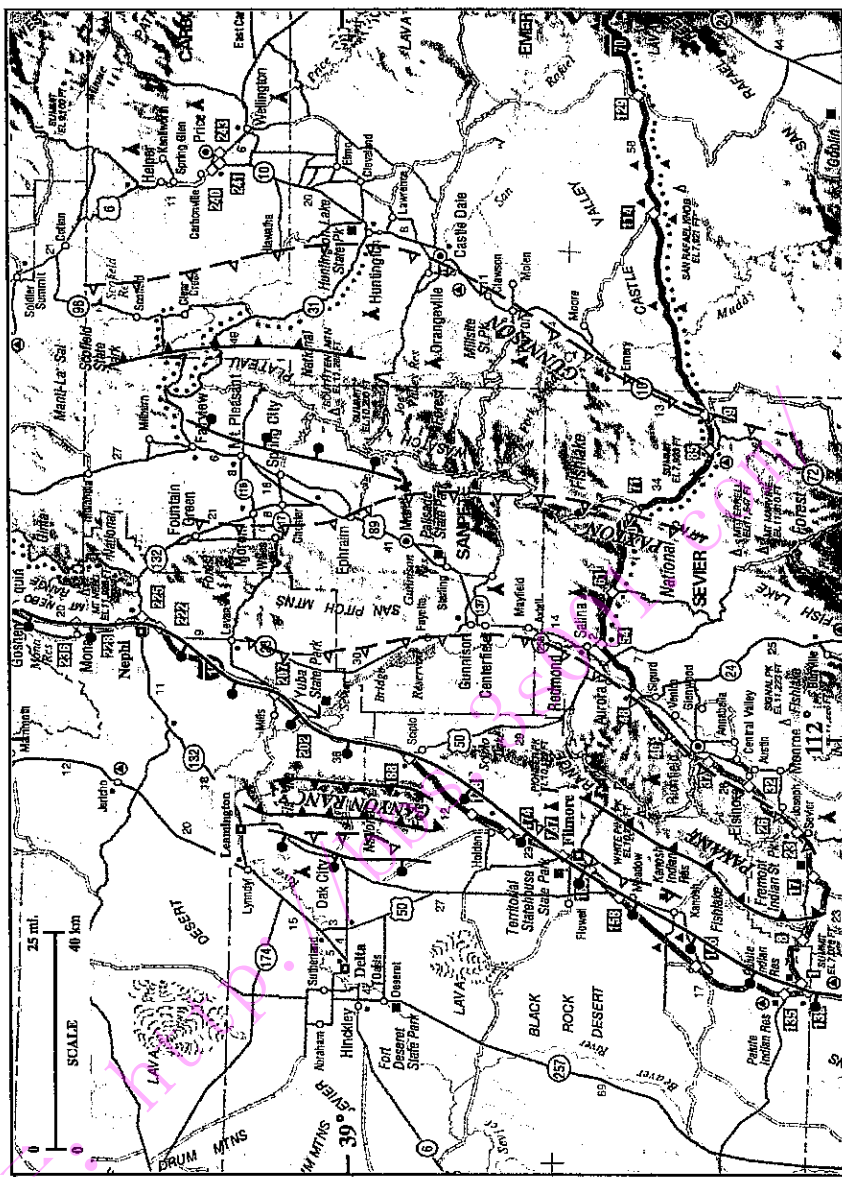
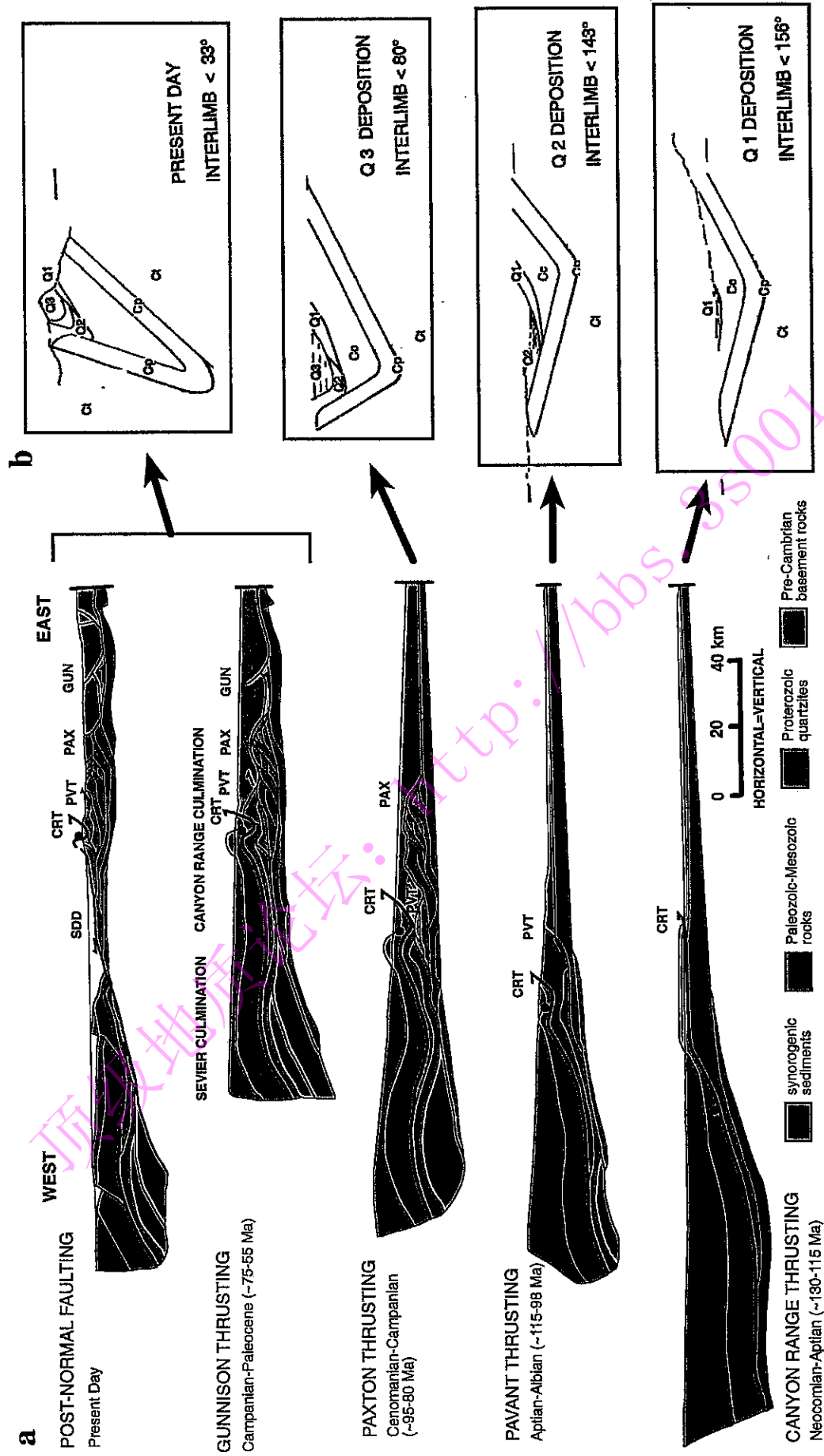


Figure 2. (a) The Sevier FTB of western USA; part b) indicated by boxed area. (b) Central Utah segment of the Sevier FTB showing the four main thrusts within the segment. The Canyon Range (CR) thrust is highlighted in red (from Ismat and Mitra, 2005).



(b) Geometry of the core of the syncline (Cambrian Pioche quartzite/shale and synorogenic conglomerates) is enlarged and illustrates the schematic unfolding history of the CR syncline (based on successive angular unconformities of the conglomerates) (from Mitra & Sussman, 1997).

Figure 3. (a) Kinematic history of the central Utah segment, Sevier FTB, with incrementally restored regional cross sections. Black dots indicate location of rocks studied through time (from Ismat and Mitra, 2001a).

tightening occurred under shallow crustal conditions (<5 km depth), i.e., within the elasto-frictional regime. In other words, because the Canyon Range syncline primarily deformed at temperatures and pressures less than greenschist grade, cross-cutting and overprinting relationships are well preserved at all scales. So, its folding history can be unraveled by tracking fracture patterns and other structures formed within the elasto-frictional regime. Third, the synorogenic conglomerate provides temporal “snapshots”; during several episodes of deposition, the conglomerates also folded and fractured as the syncline tightened.

A variety of structures are preserved from the macro- to the micro-scale throughout the fold's core. These structures have been carefully analyzed in order to answer the following questions regarding fold-tightening mechanisms. (1) How can elasto-frictional mechanisms, e.g. fracturing and cataclastic flow; produce a “ductile” structure, i.e. a fold? (2) Where, at what scales, and during what stages of fold-tightening did fracturing and cataclasis take place? (3) Did these space-problem accommodating structures all form at the same time? (4) How do these structures vary from the hinge zone area to the limbs? (5) Did the hinge migrate, and if so, did the pin's position vary from the inner arc to the outer arc of the fold?

Deformation patterns were studied both in the field and laboratory. The collected data was then synthesized to develop a more complete detailed kinematic history of the Canyon Range syncline. More specifically, I mapped macro-scale patterns from photographs I took from an airplane, along with topographic and U.S. Forest Service aerial photographs. I analyzed fracture patterns and other features preserved throughout the core (fifty-seven sites) at the outcrop (meso-) scale. Fracture patterns and the characteristics of the cataclasized rocks were also analyzed at the micro-scale from thin sections made from oriented samples collected from over thirty of the fifty-seven sites. I have developed unique methods for analyzing these rocks at

the micro-scale, which may hold critical clues to deformation within the elastico-frictional regime.

Geology

Regional Geology

The Sevier Fold-Thrust Belt (FTB), part of the Cordilleran mountain range, trends north-south through western North America (Utah, Wyoming, Montana, and Idaho) and is subdivided into salients and segments separated by recesses and transverse zones (Fig. 2). The Central Utah segment is the type area of the Sevier FTB (Fig. 2) (Christiansen, 1952; Armstrong, 1968; Mitra, 1997). From west to east, the four major thrusts found within the Central Utah segment are: the Canyon Range (CR), Pavant, Paxton, and Gunnison thrusts; the rocks that they carry are referred to as the Canyon Range, Pavant, Paxton, and Gunnison *thrust sheets*.

The Sevier orogeny occurred from the late Jurassic to the early Cenozoic (Fig. 3) (Lageson and Schmitt, 1995). Motion along the Canyon Range Thrust began ~130 Ma (Mitra 1997). The Pavant, Paxton, and Gunnison thrusts followed, forming at ~ 115 Ma, 95 Ma, and 75 Ma, respectively (Fig. 3a), (Christiansen, 1952; Armstrong, 1968; Allmendinger et al., 1983; Holladay, 1983; Millard, 1983; Villien and Kligfield, 1986; Pequera et al., 1994; Coogan et al., 1995; DeCelles et al., 1995; Mitra, 1997).

The Canyon Range thrust sheet is an internal thrust sheet in the Central Utah segment. Motion along the Pavant, Paxton, and Gunnison thrusts reactivated the Canyon Range thrust and progressively folded the Canyon Range thrust sheet into an anticline-syncline pair; this fold pair defines the Canyon Range (Fig. 3). These sheets carried by Sevier age thrusts were later broken up by Tertiary Basin and Range normal faulting (Figs. 2 and 3a). Sevier age structures, such as

folds, are well preserved in these normal-fault bound ranges, such as the Canyon Range (Fig. 2) (Ismat and Mitra, 2001a).

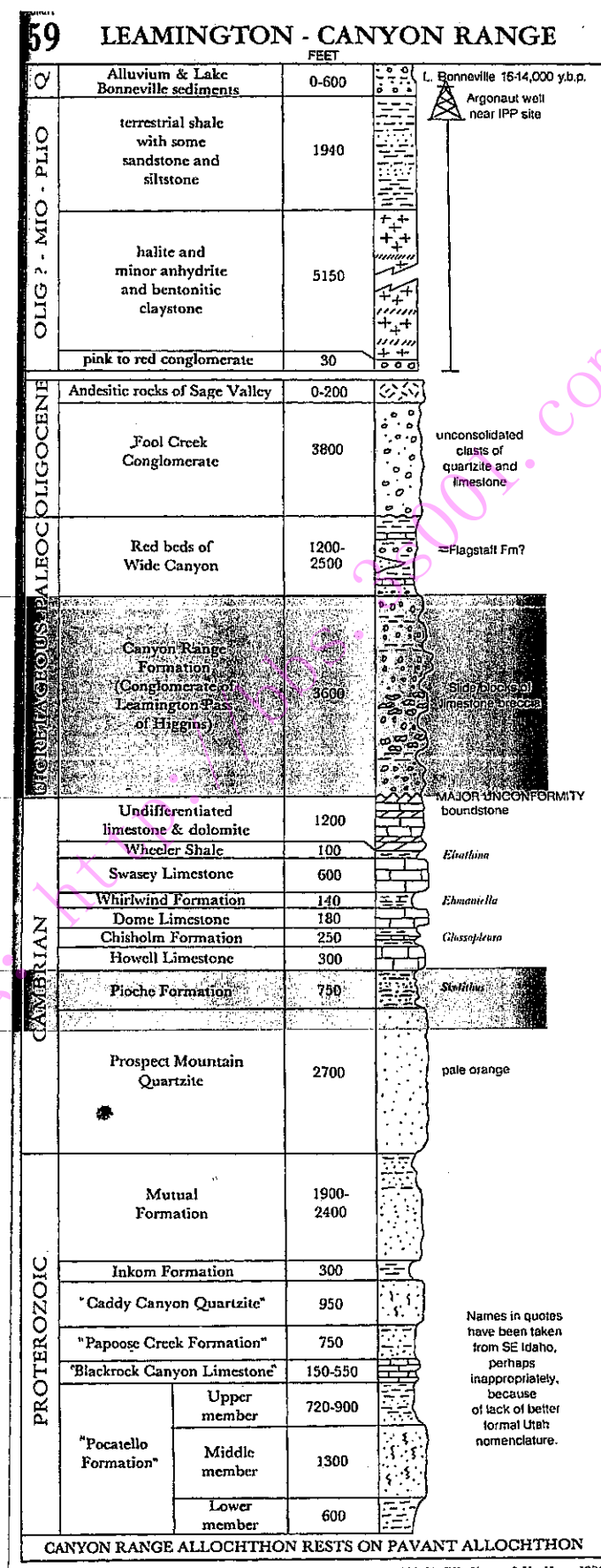
Stratigraphy of Canyon Range Thrust Sheet

The Canyon Range syncline consists primarily of Proterozoic and Cambrian quartzites (Figs. 3a and 4). Cambrian carbonates were deposited above these quartzites. The major quartzite units within the Canyon Range thrust sheet are the Neo-Proterozoic Pocatello (PCp), Caddy Canyon (PCc), and Mutual (PCm) Formations, the Eocambrian Tintic Formation (Ct) (lower, middle, and upper), and the Cambrian Pioche Formation (Cp) (Fig. 4), (Hintze, 1988; Ismat and Mitra, 2005). Synorogenic Cretaceous conglomerates (CR conglomerates) are deposited unconformably in the core of the syncline, i.e. on top of the Cp unit and the Cambrian carbonates (Fig. 3b). The carbonate units taper out and/or are missing due to a fault (Mitra, personal communication, 2005) in the hinge region; I studied the part of the core where the synorogenic conglomerates were deposited unconformably on top of the Cp unit.

The Cp is a quartzite-phyllite interbedded unit. There are two primary quartzite layers, separated by a phyllite layer, exposed in the CR syncline. Characteristic *Skolithos* worm tubes are found throughout the Cp quartzite layers. In contrast, the Ct has worm tubes only in its upper part; this distinguishing characteristic was used to differentiate between the two units (Fig. 4). The core of the syncline is defined by the upper Ct, the Cp and the CR conglomerate (Figs. 3b and 4); this paper focuses on these three formations, where much of the deformation is localized and well exposed.

Figure 4. Stratigraphic column of formations exposed in the CR syncline. Red highlighted areas are formations exposed in the core of the CR syncline (Hintze, 1988).

Formations studied



The Canyon Range trends approximately north-south and is composed of an anticline-syncline pair – the west limb of the syncline and the east limb of the anticline are a common limb (Fig. 3a). This fold pair formed with an overall east-west, sub-horizontal shortening direction (Ismat and Mitra, 2001a). The Canyon Range thrust sheet carries Proterozoic quartzites to the surface, placing them above strata ranging in age from Cambrian through Devonian (Christiansen, 1952; Millard, 1983; Holladay, 1984; Lawton et al., 1997; Ismat and Mitra, 2001a).

The Proterozoic quartzites began deforming with initial thrusting at a depth of ~15 kilometers (Fig. 3a), (Ismat and Mitra, 2001a). As the CR sheet moved over a ramp in the Pavant thrust, it started folding (Fig. 3a). Much of the fold-tightening took place during the later part of the Sevier orogeny at a depth of ≤ 5 kilometers, which includes ~ 2 kilometers of overlying synorogenic CR conglomerate. This continued erosion and uplift carried the CR sheet into the elasto-frictional (EF) regime. Because of its shallow depth (i.e., within the EF regime), fracturing and cataclastic flow accommodated much of the CR syncline fold-tightening.

The core of the CR anticline is composed of a connecting splay duplex, which formed and was continuously reactivated due to motion on younger thrusts (Fig. 3a). The duplex's growth caused the Canyon Range anticline to be uplifted and become a local culmination (Mitra and Sussman, 1997). At the same time, the anticline-syncline pair tightened (Fig. 3a). As the local culmination grew, sediments eroded from the anticline and were deposited unconformably into the core of the adjoining syncline, forming the CR conglomerate (Fig. 3b) (Millard 1983, Holladay 1984, Hintze 1991, Lawton et al. 1997). Since these conglomerates were deposited during fold-tightening, they are also tightly folded and fractured. The variation and style of

folding of the different conglomerate layers are used to track the folding history of the CR syncline (Fig. 3b).

The number of horses, the size of the horses, and the motion along the thrusts within the duplex vary along the length of the range. Similarly, the geometry of the syncline varies along its length. At its southern end, the syncline is an open, non-plunging fold; at its northern end, the fold is a tight, overturned fold plunging at least 45° to the NNW (Ismat and Mitra, 2001a). From south to north, the west limb progressively becomes steeper until it eventually is overturned. In the south, the interlimb angle is 156° , while in the north, the interlimb angle is as small as 33° (Mitra and Sussman, 1997; Ismat and Mitra, 2001a). Hinge migration, and thinning and stretching of the overturned west limb accommodated much of the fold-tightening (Ismat and Mitra, 2001a, 2005).

Canyon Range Syncline

The core of the Canyon Range syncline is well-exposed at the northern end of the range. Fortunately, this is where most fold-tightening occurred, and therefore, the most complex structures developed. Some of these fold-tightening related structures include parasitic folds associated with motion on the CR thrust, bed-parallel flexural slip and hinge migration, out-of-the-core thrusts, and bed thickness changes from the hinge to the limb.

The synorogenic conglomerate is deposited unconformably on top of the Cp quartzite and is best preserved at the northern end of the range. Not only did the quartzite beds fold by elasto-frictional mechanisms, but the synorogenic conglomerate also folded by fracturing and cataclastic flow. The contact between the fractured Cp and fractured CR conglomerate is well exposed on the west side of the hinge region (Fig. 3b). An intraformational conglomerate

composed of fractured and cataclasized Cp quartzite is found along this contact close to the hinge zone.

Cataclastic Flow

Cataclasis involves fracturing and sliding along fracture-bound clasts, or “blocks”. If this fracturing and sliding is penetrative and deforms a body of rocks in a ductile manner (i.e., the deformed rock mass *flows*), the deformation is then referred to as cataclastic *flow*. Clearly “brittle” behavior, such as fracturing, does not preclude ductile deformation. Because of this ambiguity in terminology, we refer to cataclasis and cataclastic flow as a type of *ductile* deformation that takes place by elastico-frictional mechanisms, i.e., within the elastico-frictional regime. It is better to discuss the origin of different structures in terms of deformation mechanisms rather than behavior.

Cataclastic flow is traditionally defined for deformation at the micro-scale as “a process of deformation that involves continuous brittle fracturing of grains in a rock, with attendant frictional sliding and possibly rolling of the fractured particles past one another” (Twiss and Moores, 1992), and is typically assumed to not account for a significant portion of the deformation. Moreover, it is assumed that cataclastic flow requires a significant amount of matrix in order for the fractured clasts/blocks to slide past one another. However, cataclastic flow is capable of producing large amounts of deformation and can occur at a wide range of scales, with or without matrix. Non-matrix supported cataclastic flow can be referred to as “block-controlled” cataclastic flow (Ismat and Mitra, 2001a, 2005). Both types of cataclastic flow, however, may work together in a *cooperative*, rather than *fractal* relationship.

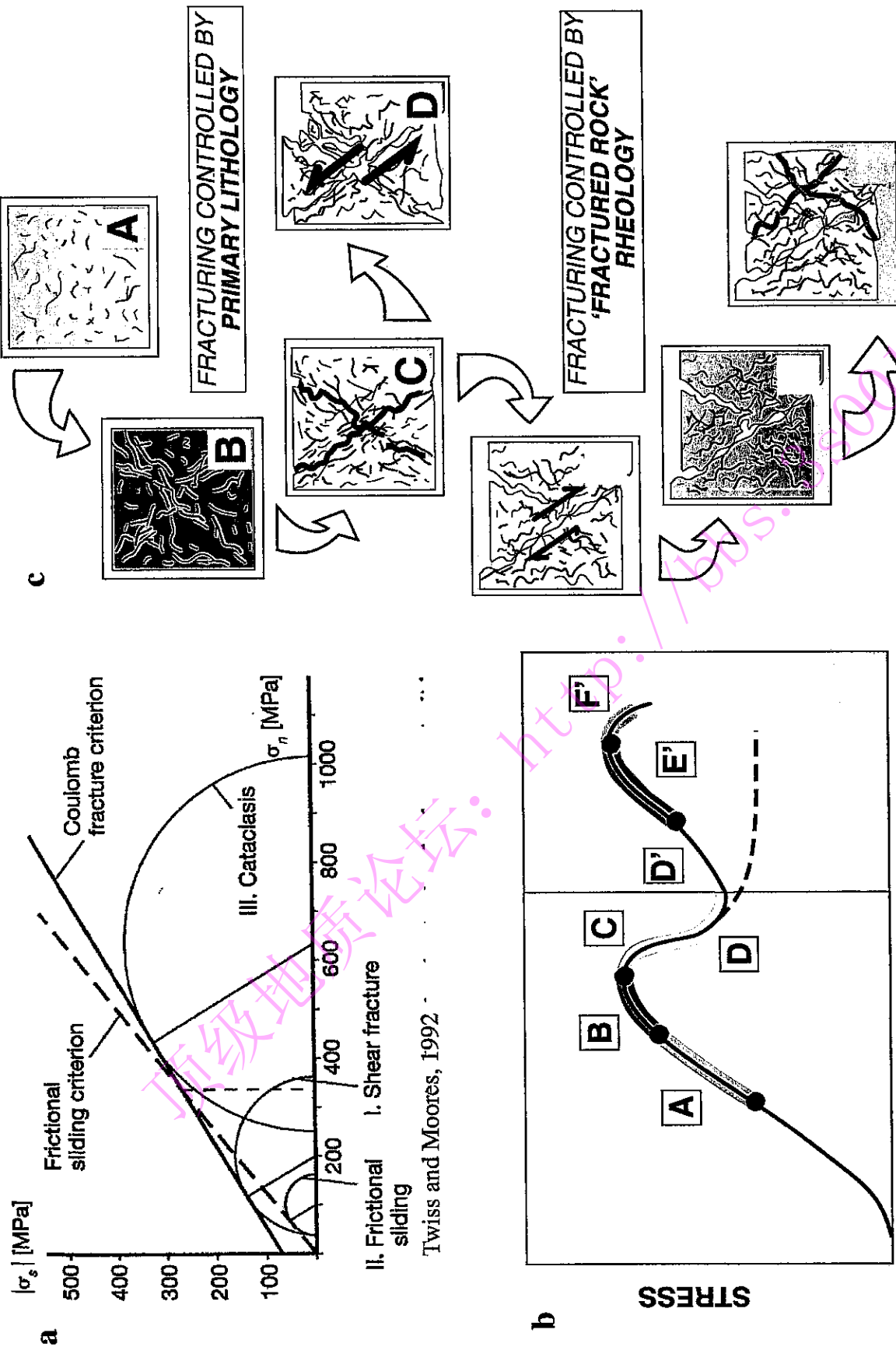
In matrix-supported cataclastic flow, the clast size progressively decreases with continued deformation. In block-controlled cataclastic flow, however, the fracture bound block size can increase or decrease during deformation (Fig. 5). Cataclastic flow cycles between fracturing and then sliding along all or some of these fractures. At each stage of frictional sliding, new and/or older reactivated fractures may be used (Twiss and Moores, 1992). Throughout the deforming material, different areas may be fracturing and sliding, and at different scales (Fig. 5). In other words, there is a cooperative relationship across all scales. The shape of these fracture bound blocks may change with increased stages of deformation. The blocks may also rotate and their size may change. Clearly cataclastic flow is possible at a range of scales, and this allowed the Canyon Range syncline to deform in a ductile manner, i.e. *fold*, by fracturing, a “brittle” process.

Data Collection

To truly understand deformation mechanisms, structures and features were studied and documented at the macro-, meso-, and micro-scales.

Macro-scale Structures

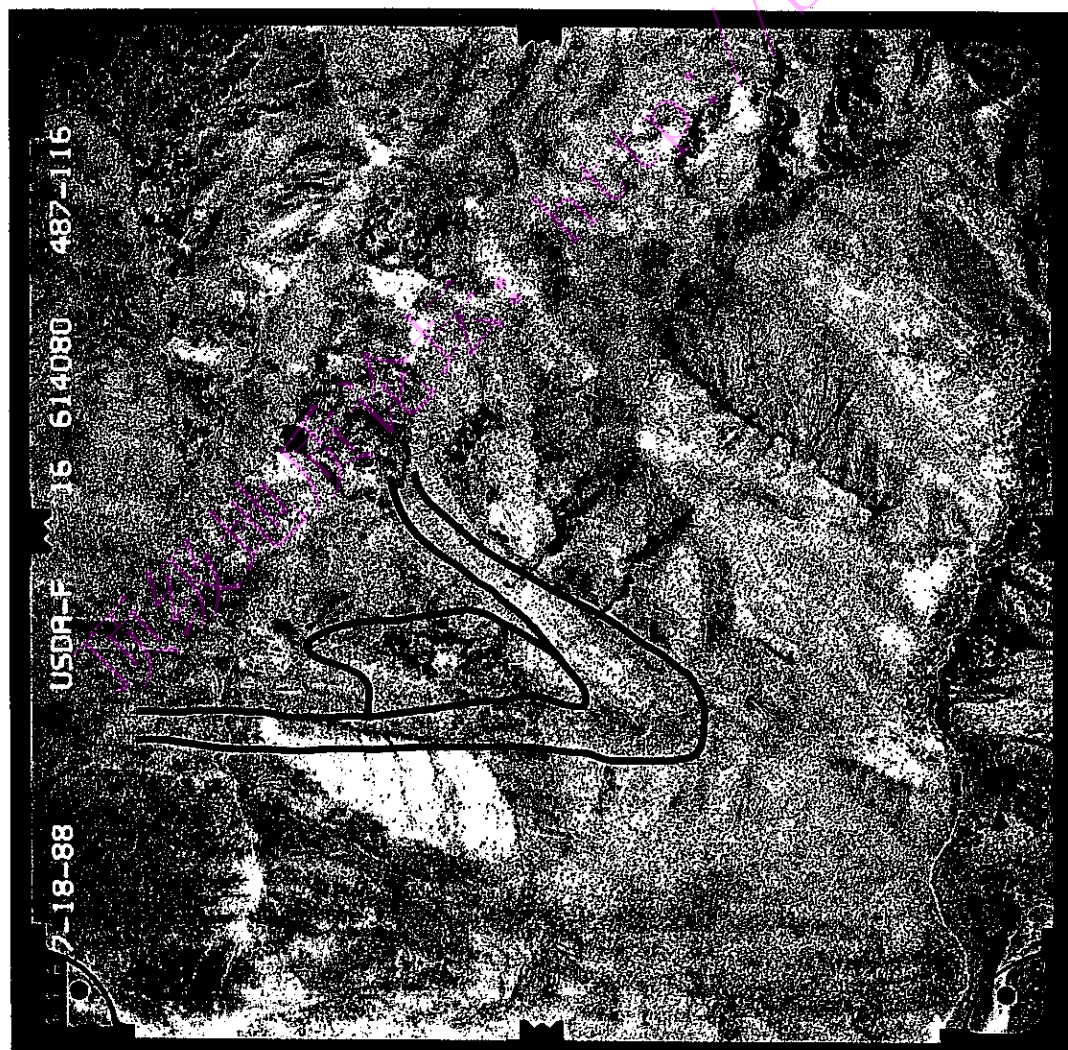
1:24,000 topographic maps and published U.S. Forest Service aerial photographs were used to locate field sites and map macro-scale patterns (Fig. 6). The resolution in these maps is too low to accurately trace out some structures and contacts recognized on the ground. Because of this, I flew over the CR syncline in a crop duster (Pilot: Zane Crafts) and took photographs of



STRAIN

Figure 5. (a) Mohr circle for Coulomb fracture criterion (solid line) and for frictional sliding on an existing fault surface (dashed line). Circle I: the critical stress necessary for shear fracturing, II: the critical stress for frictional sliding on a fracture plane, and III: the critical stress for cataclastic flow during which fracturing requires a lower differential stress than frictional sliding (from Twiss and Moores, 1992). (b) A schematic rheology graph showing the evolution of shear fracture development (from Ismat, 2002). (c) A series of diagrams depicting the evolution. In stages A-D, primary lithology controls deformation, while in stages D'-F', fractured rock rheology controls deformation (this is indicated by the shaded background in both (b) and (c)). A - a sample with micro-fractures. B - Micro-fractures grow and link up with other fractures. C - Growth of micro-fractures leads to development of meso-scale fractures. Conjugate fractures form 30 degrees from the compression directoin. Once these fractures form, deformation can continue in a cyclic manner by D - sliding along the fractures during strain-softening or fractures lock up and new micro-fractures form (D'-F', during strain-hardening (from Ismat, 2002)).

a



b

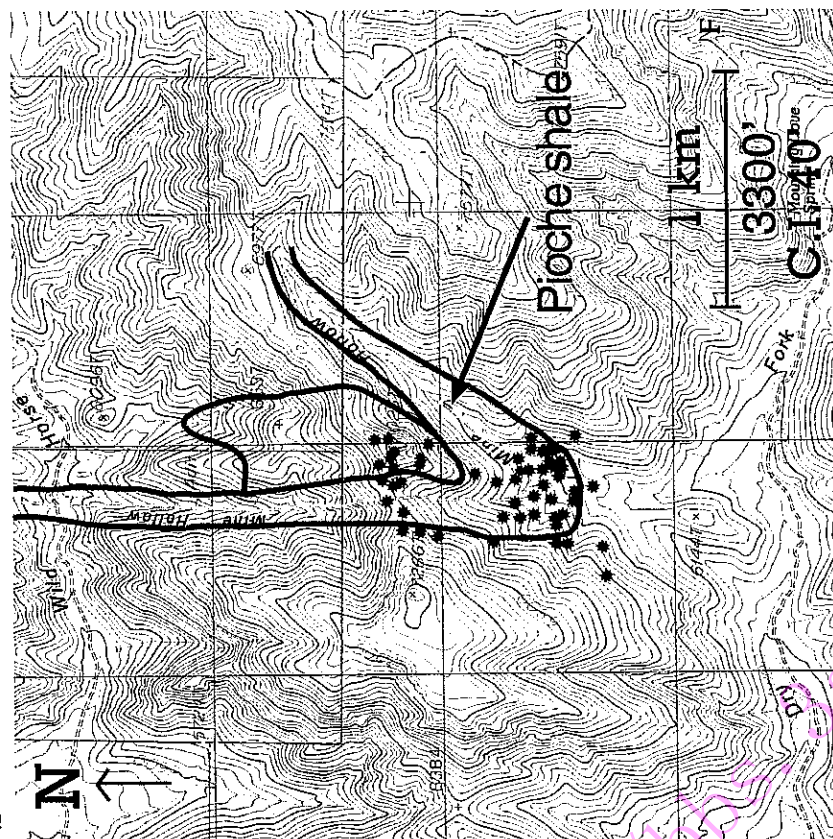


Figure 6. (a) Aerial photograph and (b) topographic map (at same scale) of the CR syncline's core (Pioche quartzite/shale and synorogenic conglomerates). Dots on topographic map show locations where detailed analysis was conducted. Note z- fold in aerial photograph (defined by shear arrows) and the shale boundary between the two quartzite layers within the Pioche.

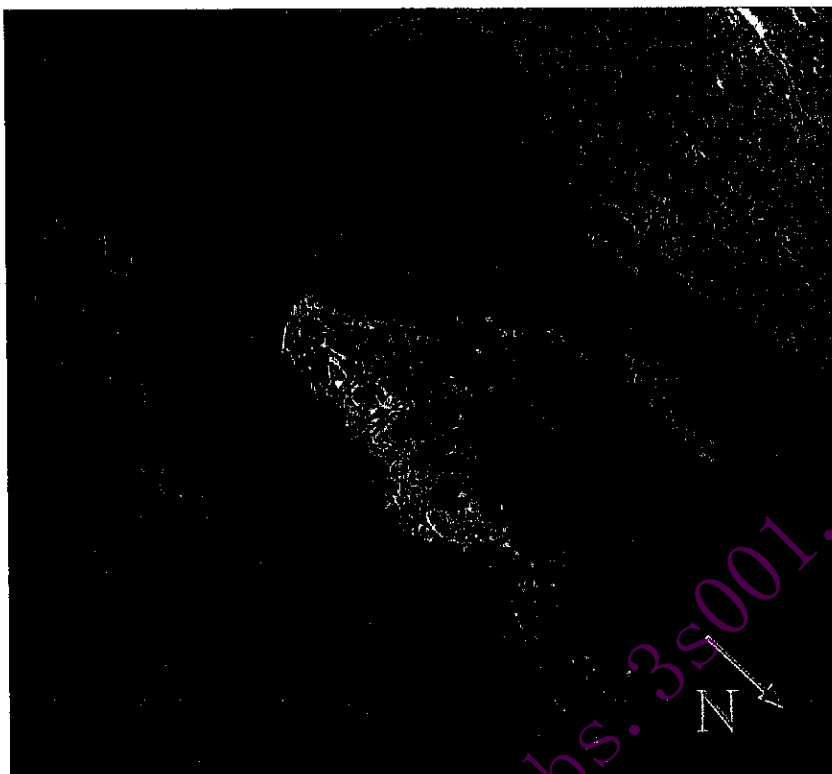
the core and surrounding area (Figs. 7 and 8). These photographs are at a resolution between the 1:24,000 scale and the outcrop-scale. They were used in conjunction with the topographic map and published aerial photographs to more completely map out macro-scale structures, patterns, and contacts, such as parasitic folds, fold-related faults, and geometry of the folded Cp unit and conglomerate layers.

The Ct/Cp contact and the Cp/CR conglomerate contact are labeled on the topographic map, published aerial photographs and airplane photographs (Figs. 6-9). Fold-related faults and a detailed geometry of the folded CR conglomerate are well expressed and highlighted in these crop-duster photographs (Fig. 9), as are the fracture patterns within the conglomerate (Fig. 10). From a U.S. Forest Service published aerial photograph, a parasitic z-fold is easily recognizable in the east limb within the Cambrian Tintic, close to the Tintic/Pioche boundary (Fig. 6a).

Meso-scale Structures

Within the Canyon Range syncline, detailed field analysis was conducted at fifty-seven sites in the Tintic quartzite (Figs. 6 and 8), the Pioche quartzite, and the Cretaceous CR conglomerate; numbered sites indicate locations discussed in this paper (Fig. 8). At each site, a rock sample was taken, and fracture patterns, orientation of bedding, and orientation of *Skolithos* were recorded. Because fold-tightening occurred primarily by thinning and stretching of the rotated west limb, many of my sites were purposely chosen in the west limb (Figs. 6 and 8). The hinge of the fold was studied at sites 19-24 (Fig. 8). I also collected data from a transect across the east limb into the core (Site 4), (Fig. 8), to see how the deformation changed from the limb to the core, i.e., did the fracture patterns continue into the conglomerate from the Cp, did they

a



b

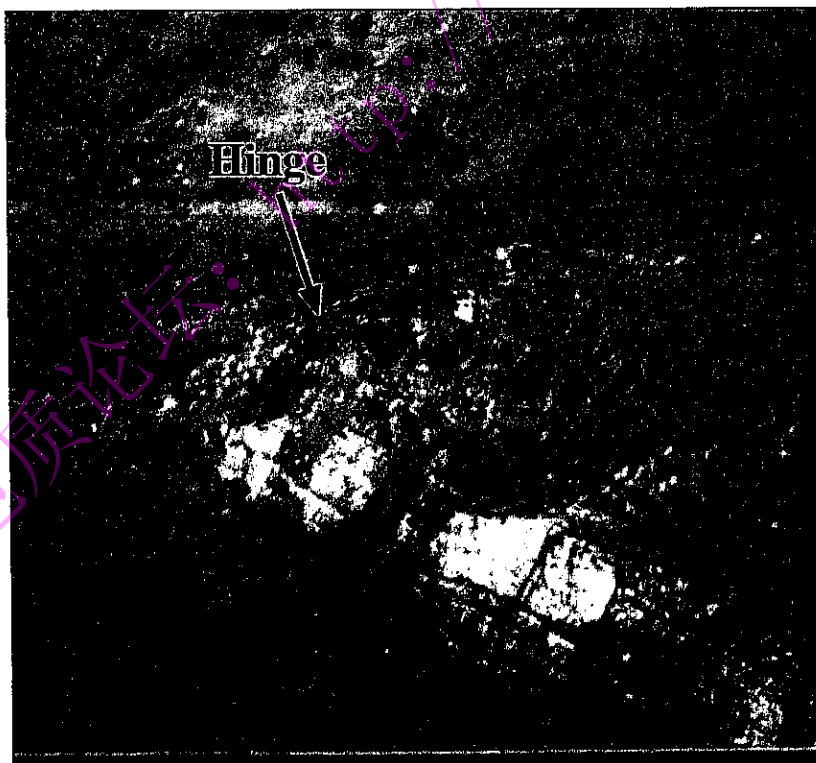


Figure 7. (a) CR syncline viewed from the air. (b) Photograph taken of the hinge region of the Pioche.

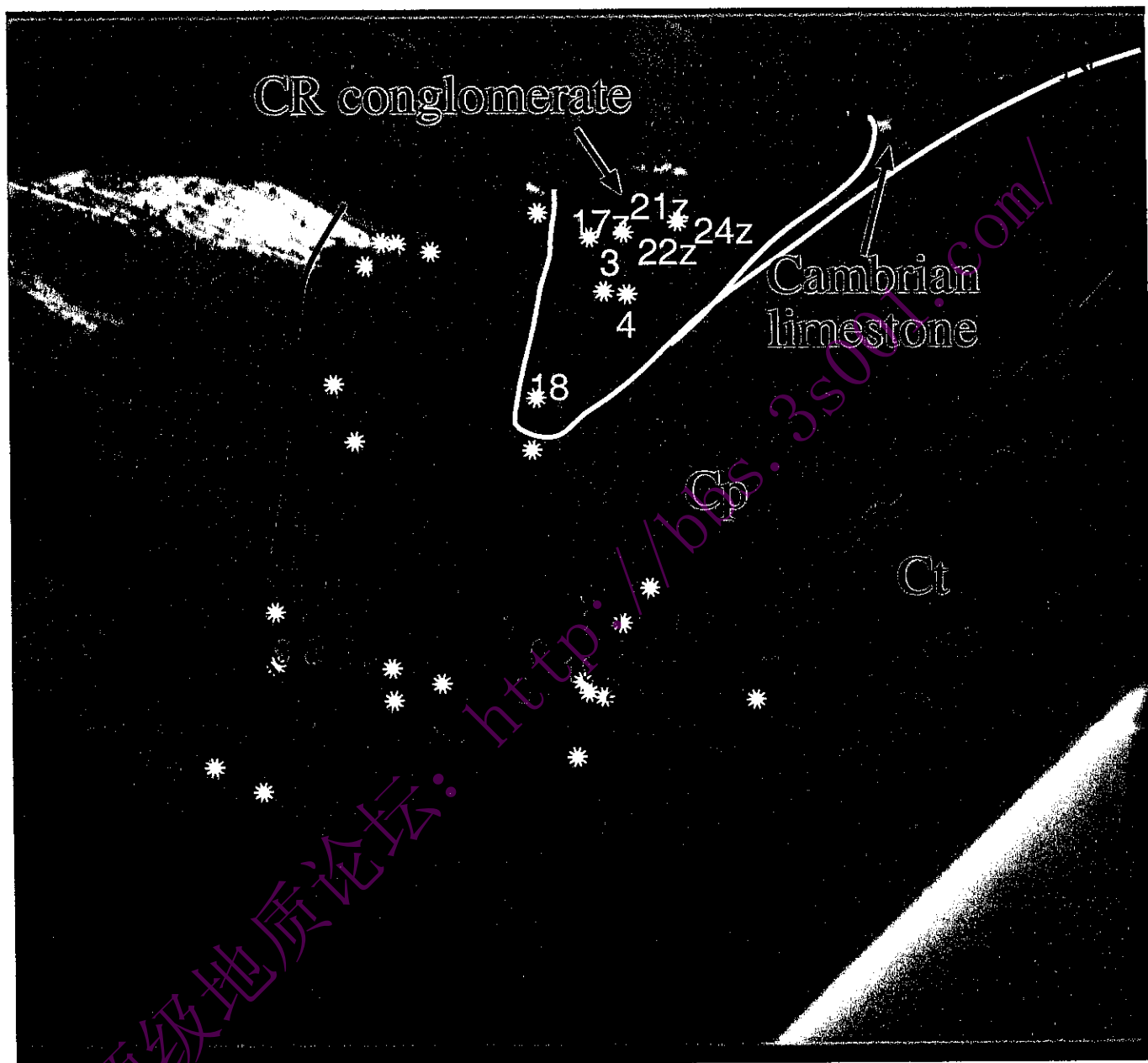


Figure 8. Aerial view of the CR syncline's core, looking north. Dots show locations where detailed fracture analysis was conducted and/or samples collected. Numbered sites indicate locations discussed in this paper.

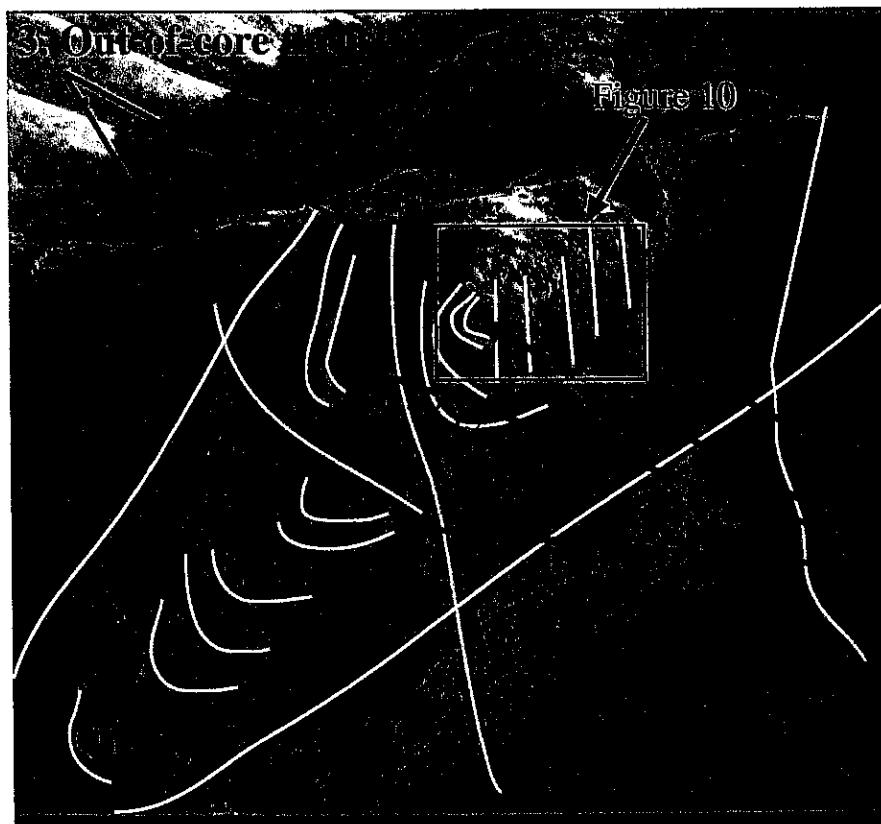
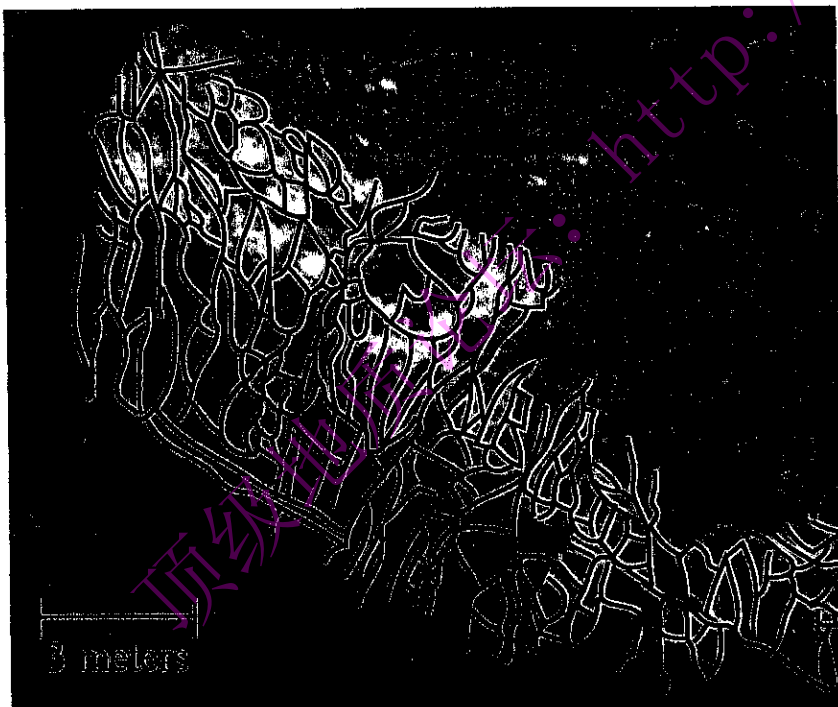


Figure 9. 1. The east-west trending faults cross-cut all the earlier fractures. They most likely formed during the late stages of fold-tightening, when the limbs were relatively steep. 2. Evidence for hinge migration is preserved in the folded synorogenic conglomerates; note how the hinge in the upper layers progressively rotate into the west limb. 3. Out-of-core thrusts form to relieve space problems in the core of the fold. 4. Large faults refracted as they propagated through different lithologic units (quartzite, limestone and conglomerate). Q1 - Q3 represent different depositional layers of the conglomerate (Q1 is the oldest).

- 1. East-west trending faults
- 2. Folded conglomerate
- 4. Refracted faults

a



b



Figure 10. (a) East wall (looking west) of the synorogenic conglomerates. Fracture traces highlighted with black lines. Note high density of fractures (see Fig. 9). (b) Steep E-W trending fractures are prominent in the conglomerate and cross-cut all earlier formed fractures. These most likely formed in the late stages of fold-tightening with an overall E-W sub-horizontal shortening direction (see Fig. 9).

refract, and did they change in density and variation in other small-scale structures? Several features were very noticeable at this scale that had not been evident at the macro-scale.

In addition to detailed fracture analysis, data was collected on other meso-scale structures, such as parasitic folds. An s-fold (facing north) was found in the east limb at Site 29 (Figs. 8 and 11), and a z-fold (facing north) was also found in the west limb (Sites 5 and 6), (Fig. 8); the asymmetry for both of these parasitic folds is opposite of what is expected for both limbs of a syncline. A large synformal hinge in the older (i.e., lower) Cp quartzite layer is well preserved within the east limb of the CR syncline (Sites 19 – 24), (Fig. 8).

Micro-scale Structures

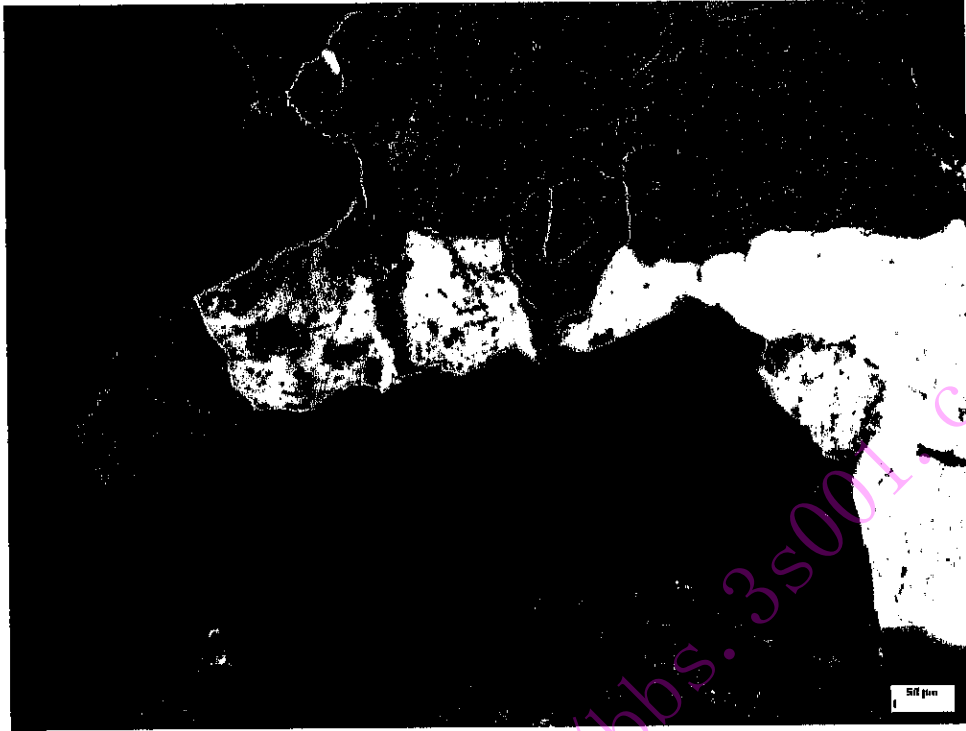
Over forty oriented samples were collected from thirty sites within the Cp quartzite. The samples were then cut for microstructural analysis. Most of the oriented samples were cut parallel to the east-west transport direction; about ten additional samples were cut along three mutually perpendicular sections (vertical east-west, vertical north-south, and top, i.e., azimuthal plane) in order to unravel the three-dimensional deformation at the micro-scale. Thin-sections were viewed in plane and polarized light and using dark field¹ microscopy. In dark field, many of the structures, such as healed fractures, that were not noticeable under cross and/or plane polarized light became visible (Fig. 12).

¹ To view slides in dark field, an opaque disc is placed below the condenser lens. This allows the light to be scattered by objects on the slide. Reflected colors appear where pigmented objects exist; other parts absent of pigmented objects are dark. Dark field is typically used at low magnifications.



Figure 11. S-fold (face striking 065) within the upper quartzite layer of the Pioche unit (quartzite interbedded with phyllite) in the east limb; its asymmetry is opposite from what is expected. The plunge of this fold is less than the plunge of the overall syncline. Both lines of evidence suggest that this s-fold formed in the later stages of folding. (Photo taken looking N 22 W).

a



b

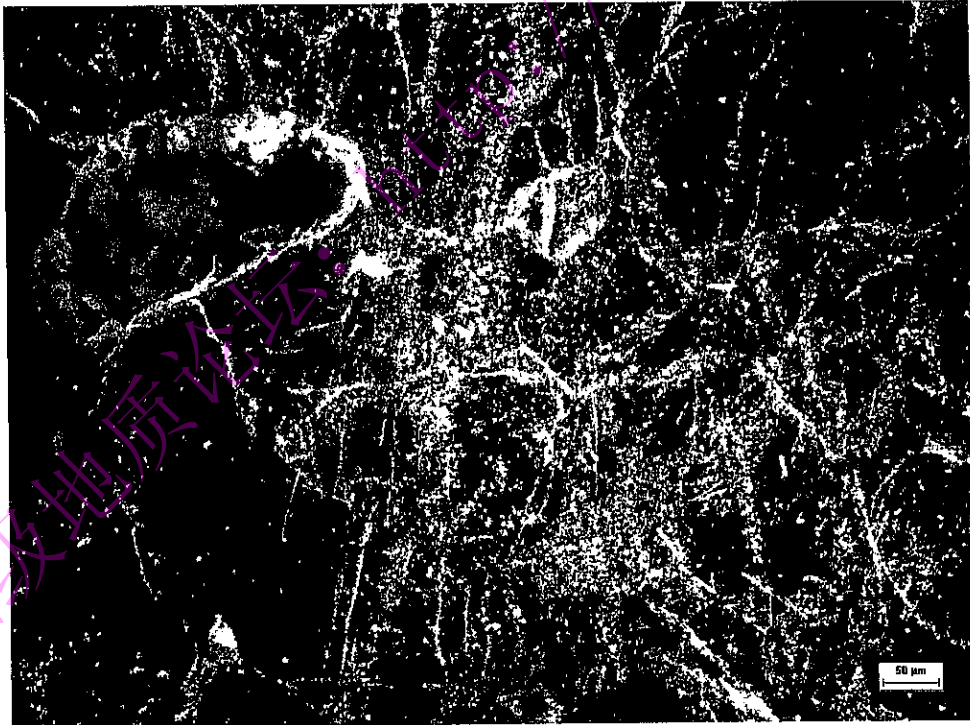


Figure 12. Photomicrographs from Pioche quartzite in both plane light (a) and dark field microscopy (b). Note healed fractures (bubble trails) and overgrowths, which are more visible under dark field microscopy.

Data Analysis

Deformation patterns were analyzed on each scale and then synthesized across all scales to understand the interactions amongst them, and the relationships across different scales.

Macro-scale Structures

Macro-scale faults preserved in the core have an overall east-west trend. In detail, the trends of thrusts change across lithologic boundaries (quartzite, limestone, and conglomerate), most likely indicating refraction during fracture propagation. Some of these faults may have formed as out-of-the-core thrusts to accommodate space problems in the core (Fig. 9). The east-west orientation of these faults may be a result of the overall east-west shortening direction and/or extension parallel to the hinge of the fold during fold-tightening.

Space problems may have also been relieved by hinge migration. Evidence for this is preserved in the folded synorogenic conglomerate. The bedding is folded, and the hinge in the older layers progressively rotates into the west limb (Figs. 9 and 13).

Along the northwest-southeast trending face of the conglomerate, three sets of fractures (oriented east-west and north-south, and S 30° W) form fault-bounded blocks ~ a cubic meter in size (Fig. 10a). The prominent, steep east-west trending fractures crosscut all earlier formed fractures in the conglomerate (Figs. 9 and 10). These steep east-west fracture sets do not continue into the adjacent Cp quartzite.

The fold axis for this part of the syncline is oriented 32°, 337°, based on over fifty bedding orientations measured at the northern end of the fold (Ismat and Mitra, 2005). The

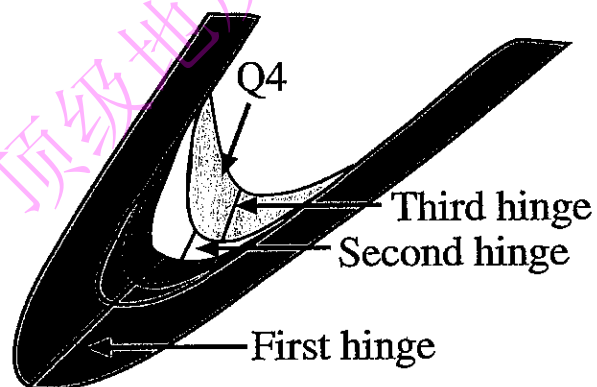
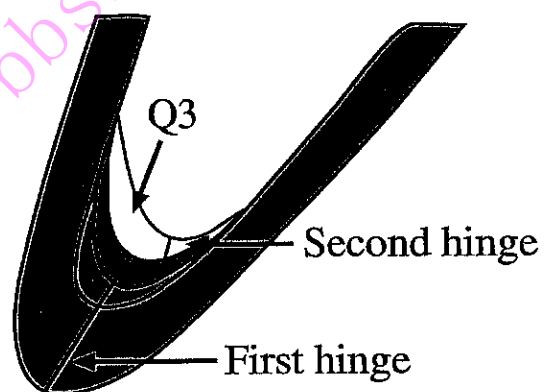
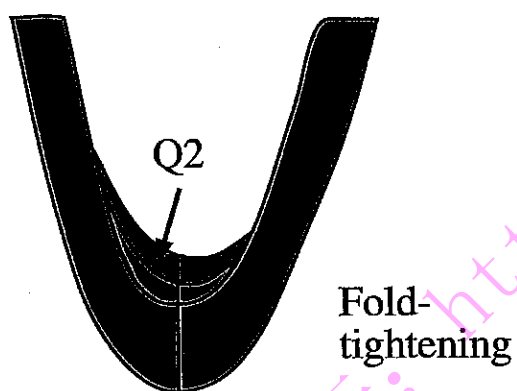
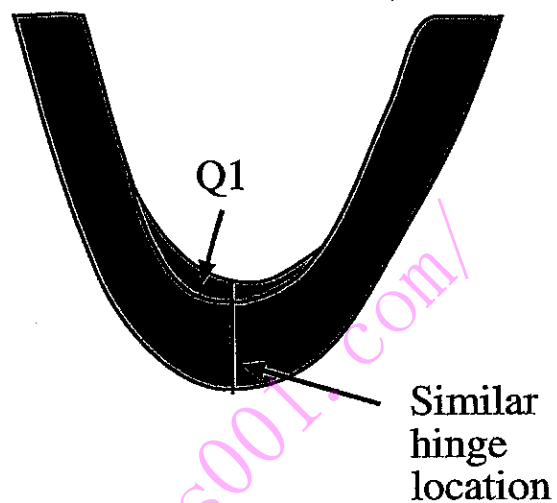
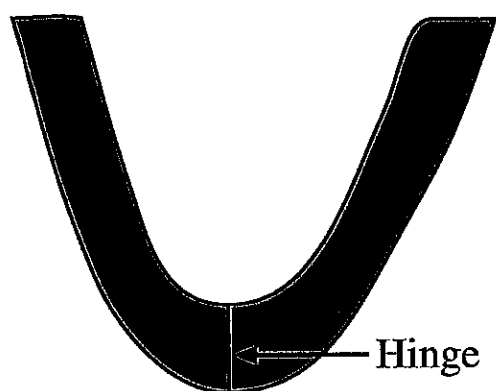


Figure 13. As the fold tightened, the hinge migrated. The different layers of the CR conglomerate recorded the fold's history by folding and preserving the path of the hinge's migration. Q1-Q4 represent different depositional layers of the conglomerate.

bedding contacts on the topographic map and the orientation of the fold were used to construct a down-plunge projection (Fig. 14). From this construction, we see that the hinge of the fold thickened by as much as ninety percent while the limbs thinned by as much as seventy percent. The deformation, however, is not plane-strain; based on an undeformed thickness of the Cp (750 feet) for this fold shape, there is ~10% material loss from this fold profile (Fig. 15).

Meso-scale Structures

Fracture data was collected at 22 of the fifty-seven sites within the upper Ct and the Cp quartzite units. The fractures are mutually crosscutting and therefore assumed to have formed at one stage of deformation (Fig. 16). In order to calculate an accurate shortening direction for that deformation stage at each site, fractures were weighted according to their frequency, magnitude and continuity within the site area (see Ismat and Mitra 2001a for a more detailed description of this method) (Fig. 17). The orientations of these fractures' poles were plotted on equal-area stereonet. From the pole concentrations, planes were plotted as great circles. Using these planes, conjugate-conjugate patterns were determined (Reches, 1983). The acute bisector of these patterns reveals the maximum shortening directions (S_3) at different sites (Fig. 16). The typical shortening direction, plotted as blue dots, for most of the sites was near-vertical (Fig. 17).

Fracture data were taken for two small-scale folds found within the hinge region of the CR syncline (Sites 5, 6, and 29, Figs. 8 and 18). The great circles for the fractures were plotted in red on equal-area stereonet (Fig. 18). The maximum shortening direction is illustrated as an orange dot on the stereograms.

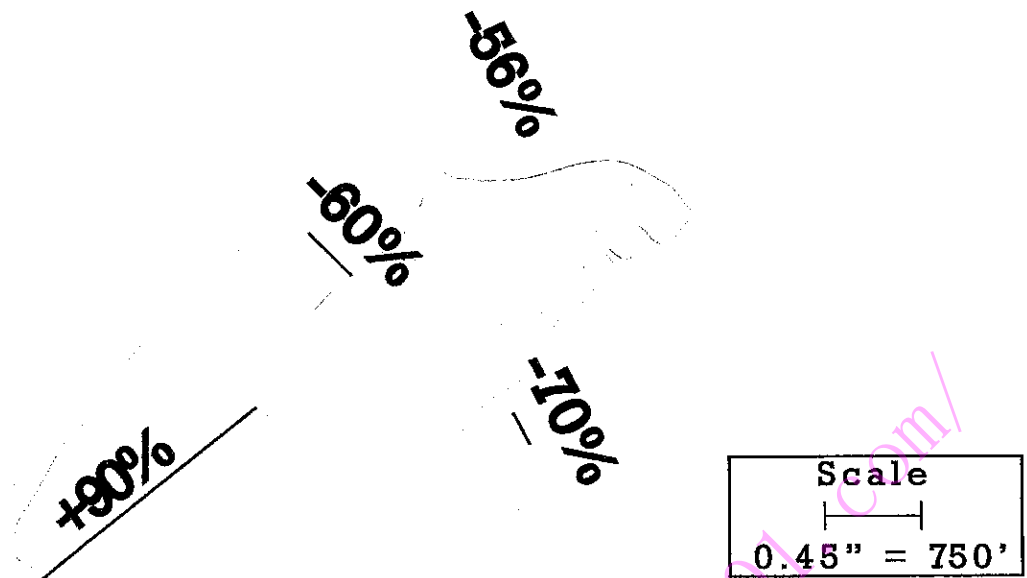


Figure 14. Down-plunge projection (looking toward fold axis (32, 337) of the Cambrian Pioche (yellow) and the synorogenic conglomerates (green) of the CR syncline. The Pioche unit in the hinge thickened by as much as 90%, while the limbs thinned by as much as 70%

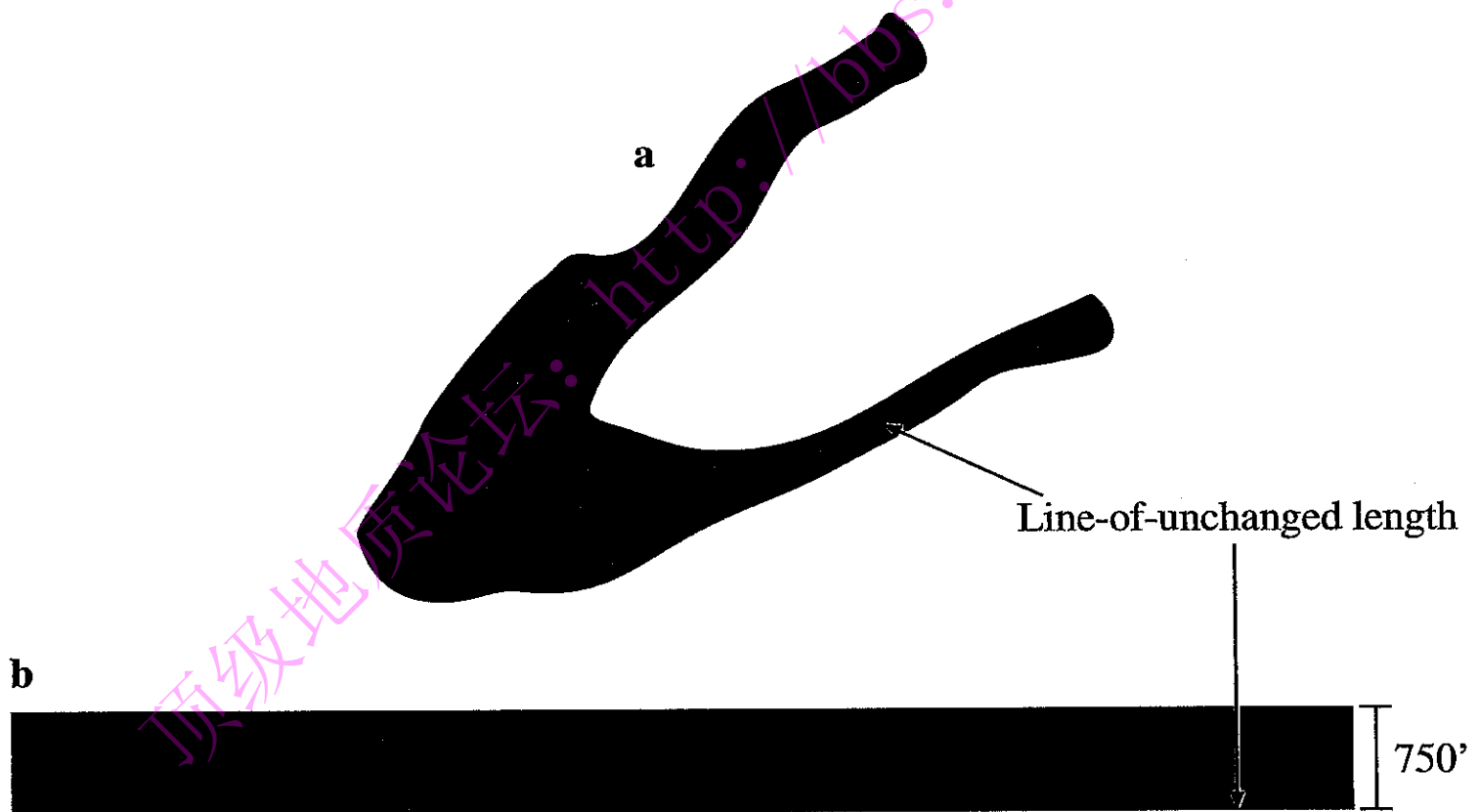


Figure 15. (a). The down-plunge projection's (DPP) area was calculated in *ImagePro Plus*. A line determined as the line-of-unchanged-length (orange line) was drawn onto the DPP. Since the fold's outer arc was stretched and its inner arc was shortened, there must be a line somewhere in the middle where the fold was neither stretched nor shortened - this is that line. (b) Using the known thickness of the Pioche unit (750'), the line-of-unchanged-length was straightened out and then a flat, horizontal bed was constructed - this represents the predeformed Pioche. The slab was 10% larger in area than the fold, suggesting that deformation was not simply plane-strain. This is a first-order approximation.

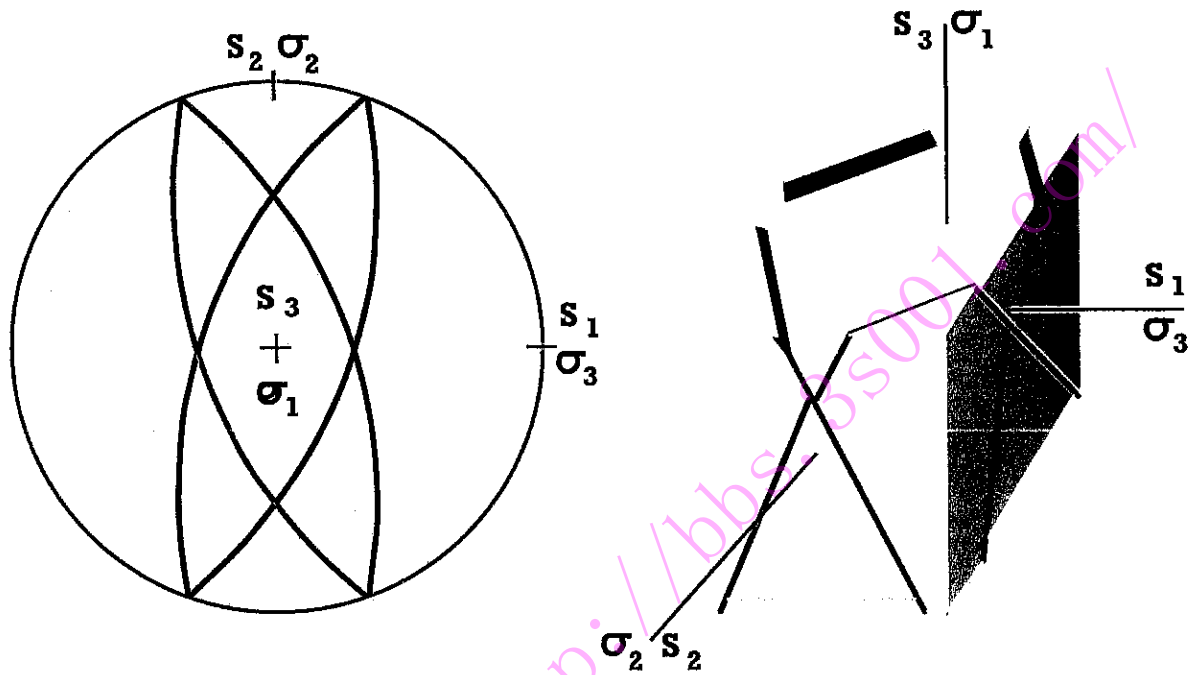


Figure 16. Fracture sets produced in a three-dimensional strain field. The acute bisector of the conjugate-conjugate sets of fractures indicates the maximum shortening direction (S3). Two-dimensional model of fracture sets produced with an E-W sub-horizontal shortening direction. As beds rotate with progressive fold-tightening, the earliest formed fractures can be passively rotated and later reactivated to accommodate limb thinning and vertical stretching. This model may explain the steep/vertical shortening directions found throughout the Pioche unit (after Reches, 1983).

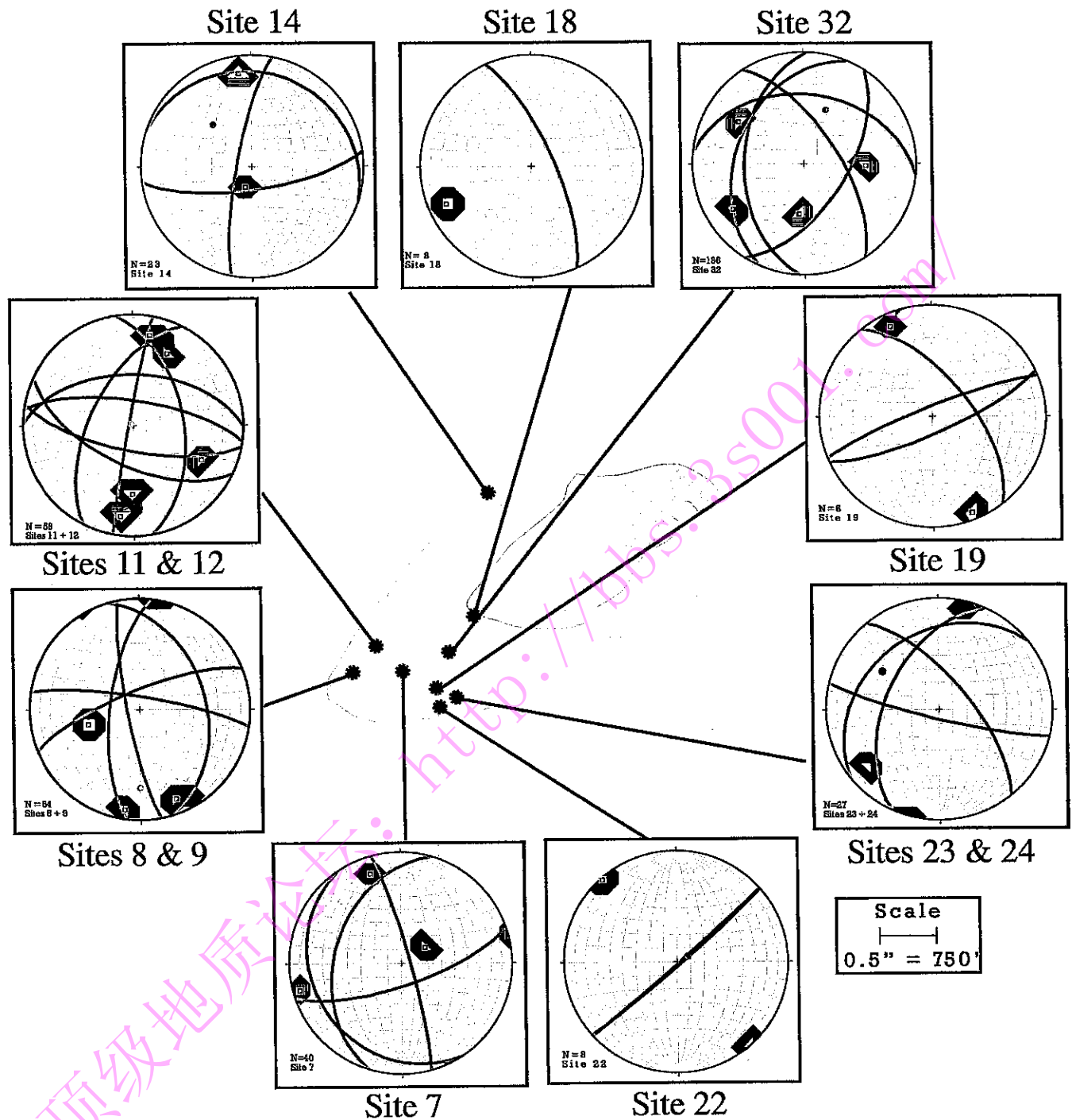


Figure 17. Blue dots indicate where detailed fracture analysis was conducted. All the fractures were measured, weighted (based on density, thickness, and continuity) and plotted as poles on equal area stereonets. The most common fracture orientations were determined from these pole concentrations and are plotted as red great circles. Based on conjugate-conjugate fracture sets, the shortening directions were determined and are plotted as blue dots. Purple great circles illustrate bedding.

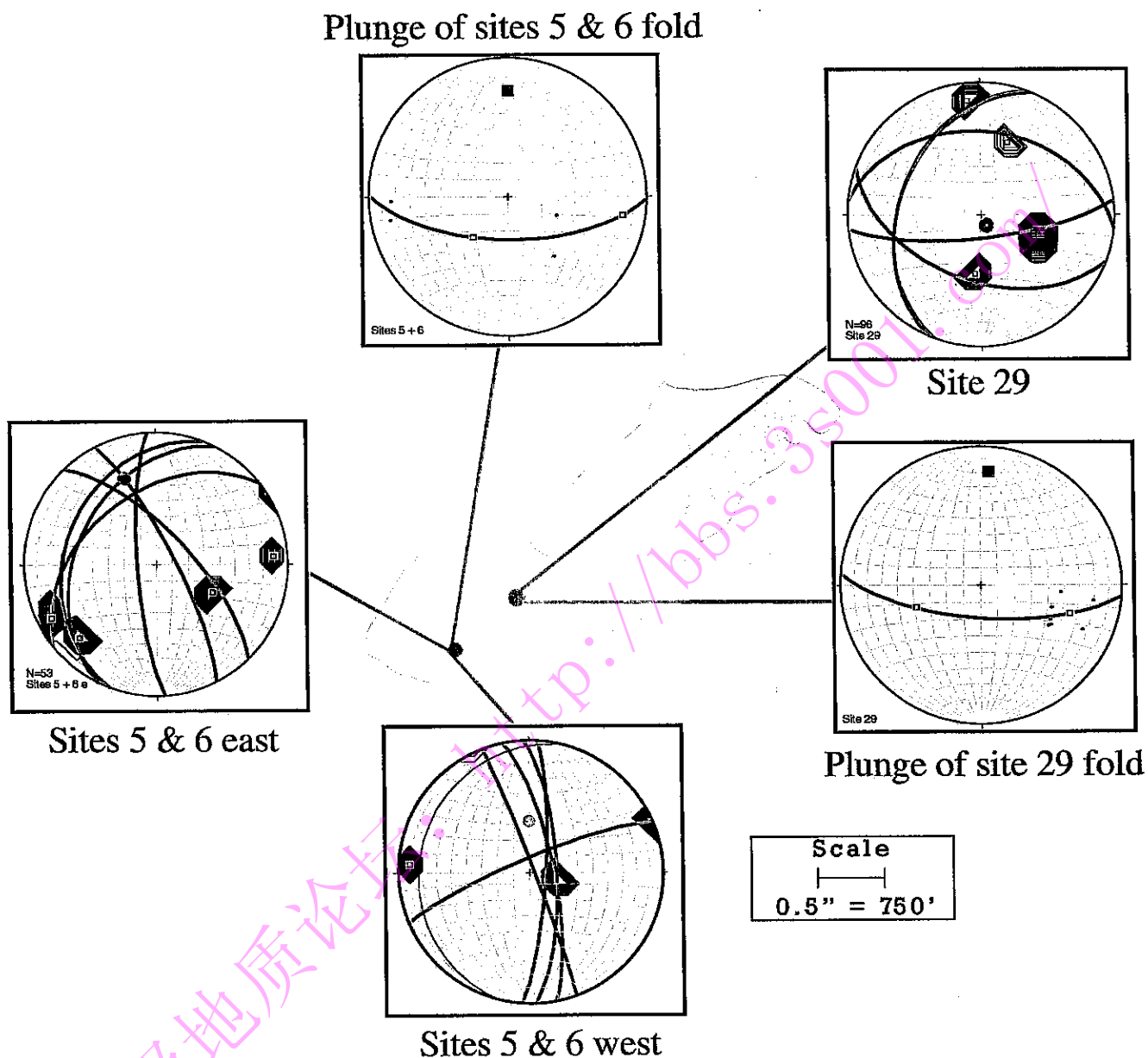


Figure 18. Fractures (red great circles) and bedding (purple great circles) plotted for two small-scale folds found within the hinge region of the CR syncline on equal area stereonets. The plunges (as shown) of both small folds are much less than the overall CR syncline, suggesting that these folds may have formed later in the folding history. The bedding poles are marked as dots on these stereograms; they were used to generate the plunge of the fold axes.

The orientations of the beds are also plotted on the stereograms as purple great circles. The bedding poles are plotted on two additional equal-area stereonets, one stereogram for each parasitic fold. A best-fit great circle was constructed from the bedding poles (Fig. 18); the pole to this best-fit great circle is the orientation of a fold's hinge and is plotted as a green square on the stereograms (Fig. 18). The plunges of both folds' hinges were $\sim 10^\circ$ due north; these plunges are much less than the 32° plunge of the Canyon Range syncline.

Slickenlines were present at five of the sites in the west limb (Sites 12z & 13z, 17z, 21z, 22z, and 24z, Figs. 8 and 19). The orientations of these lineations and their slickensided surfaces were used to construct motion planes (Fig. 19). The pole to the fracture and the lineation on that fracture defines the orientation of a motion plane; these are illustrated as black great circles. The red great circles represent common fracture orientations. The green great circles on each of the five stereograms represent the mean motion plane for that particular site; a separate stereogram contains all five of the mean motion planes plotted together (Fig. 19). The mean pole of the motion planes (10° , 358°) has a very similar orientation to the two small-scale folds' hinges' orientations. In other words, the mean pole of the motion-planes (10° , 358°) deviates from the orientation of the CR syncline in the same manner as the parasitic folds found within the hinge region of the syncline.

Micro-scale Structures

The undeformed (i.e., non-fractured) grains in the Cp quartzite have a relatively homogeneous grain size (Fig. 20). Many of the samples contained grains with overgrowth